Journal of Materials Chemistry C

ROYAL SOCIETY OF CHEMISTRY

PAPER

View Article Online
View Journal | View Issue

Cite this: J. Mater. Chem. C, 2024, 12, 1040

Cluster-induced aggregation in polyurethane derivatives with multicolour emission and ultra-long organic room temperature phosphorescence†

Nan Jiang,[a] Ke-Xin Li,[a] Jia-Jun Wang,[a] Chen-Sen Li,[b] Xiao-Yu Xu,[a] Yan-Hong Xu *[a] and Martin R. Bryce *[c]

Received 11th November 2023,
Accepted 30th November 2023

DOI: 10.1039/d3tc04141g

rsc.li/materials-c

Non-conjugated luminescent polymers (NCLPs) have the advantages of simple synthesis, optical tunability, and excellent processability. However, the underlying luminous mechanism in NCLPs remains obscure and it is a considerable challenge to obtain NCLPs with ultra-long phosphorescence lifetime and multicolour emission simultaneously. In this article, linear polyurethane derivatives (PUs) with cluster-induced aggregation, multicolour luminescence and ultra-long phosphorescence have been prepared by simply adjusting the reaction temperature and the reaction time. DFT calculations and molecular dynamics simulations provide elaborate microstructural information on the PUs. With the synergistic effect of abundant hydrogen bonding interactions, through-space dative bonds, short interatomic contacts and oxygen clusters various luminous clusters are formed. The energy level splitting caused by clusters with different extents of spatial conjugation endows the NCLPs with multicolour clusteroluminescence, promotes intersystem crossing (ISC), and stabilises the triplet excited state, and finally an ultra-long room temperature phosphorescence (RTP) lifetime of 0.45 s is attained. Experimental encryption/decryption models validate the potential of the PUs in information security. The results have important implications for understanding the intrinsic mechanism of unconventional luminescence in the absence of any traditional conjugative units or heavy atom effects, and they provide a new horizon for the strategic design of multicolour luminescence and ultra-long phosphorescence in NCLPs for a range of practical applications.

Introduction

Non-conjugated luminescent polymers (NCLPs) that consist entirely of non-conventional chromophores have attracted extensive research attention in the fields of optoelectronic devices,[1,2] biological imaging,[3,4] optical/chemical sensing[5,6] and other topics[7–10] due to their simple synthesis, easy modification, environmental friendliness, excellent processability and proven practical applications.[11–15] However, the emission of NCLPs is often limited to the short wavelength region, whereas it is difficult to achieve long wavelength luminescence.[16] More importantly, it is especially challenging to obtain NCLPs with ultra-long phosphorescence lifetimes.[17–19] Therefore, tunable luminous colour and long phosphorescence lifetime are targets for fundamental and practical advances.

Intersystem crossing (ISC) from singlet excited states to adjacent triplet states plays an essential role in phosphorescence.[20] However, ISC in organic compounds is generally less effective than in organometallic compounds where the metal ions play a key role. Therefore, activating ISC is a major challenge for NCLPs and is a prerequisite to obtain ultra-long phosphorescence.[21–23] There are two common ways to promote ISC: (i) large spin–orbit coupling (SOC) and (ii) small singlet–triplet splitting (ΔE_{ST}).[24,25] On the one hand, introducing electron-rich carbonyl groups and other units containing heteroatoms (*e.g.*, O, N, S, and P) can increase the charge constant, so that the S_1 of the phosphor is dominated by (n, π*) and the nearest low-lying T_n is dominated by (π, π*), thereby promoting the spin-allowed ISC[26] and obtaining ultra-long phosphorescence.[27–31]

[a] Key Laboratory of Preparation and Applications of Environmental Friendly Materials, Key Laboratory of Functional Materials Physics and Chemistry of the Ministry of Education (Jilin Normal University), Changchun, 130103, China
[b] Department of Chemistry Hong Kong Branch of Chinese National Engineering Research Center for Tissue Restoration and Reconstruction and Institute for Advanced Study, The Hong Kong University of Science and Technology Clear Water Bay, Kowloon, Hong Kong 999077, China
[c] Department of Chemistry, Durham University, Durham DH1 3LE, UK. E-mail: m.r.bryce@durham.ac.uk

† Electronic supplementary information (ESI) available. See DOI: https://doi.org/10.1039/d3tc04141g

On the other hand, due to the energy level splitting of cluster aggregates in NCLPs, more ISC channels can form, which can promote ISC and a smaller ΔE_{ST}.[32] In addition, the spatial conjugation and rigid conformation brought about by strong non-covalent interactions and short contacts in aggregate clusters[33–38] can inhibit molecular motion, bond rotation and non-radiative decay, thereby preventing the usual quenching of triplet excitons under environmental conditions.[39] However, the excellent potential of NCLPs remains to be developed for ultra-long phosphorescent materials.

In this work, cyclopropylboronic ester units are introduced into linear polyurethane (PU) backbones for the first time. A series of molecular-weight-dependent cluster multicolour-luminescent PU derivatives were obtained with identical chemical structures by simply controlling the reaction temperature and the reaction time during their synthesis (Fig. 1). The cyclopropylboronic ester units play an important role. First, electron-deficient boron atoms[40,41] should effectively promote the through-space conjugation of the lone pair electrons on the PU chains. At the same time the cyclopropyl ring can control the 3D structural rigidity of PU molecules[42–44] and limit the intramolecular rotation and vibration of the PU chains, promoting the formation of clusters and the spatial conjugation of electron clouds, giving rise to luminescence. Moreover, the stability of triplet excitons is enhanced which should prolong the phosphorescence lifetime, by analogy with aromatic materials.[45,46]

With the increase of molecular weight, the PU changes from a relatively free state to a weakly aggregated state and then to a strongly aggregated state. The latter structure can enhance the degree of spatial conjugation, thus narrowing the energy level gap and leading to a red shift in the emission. In addition, the rigid conformation caused by non-covalent interactions, such as entangling and abundant inter/intra-chain multiple hydrogen bonds, can effectively inhibit non-radiative transitions. As shown in Fig. 1, **PUB**, **PUG**, **PUY** and **PUR** emit blue, green, yellow and red fluorescence, respectively, under 365 nm UV light. Moreover, the **PUY** with the highest molecular weight and the most densely aggregated structure shows a remarkable phosphorescence lifetime of 0.45 s which (to our knowledge) is the longest lifetime for pure NCLPs reported to date (Table S1, ESI†).[17,18,47–50]

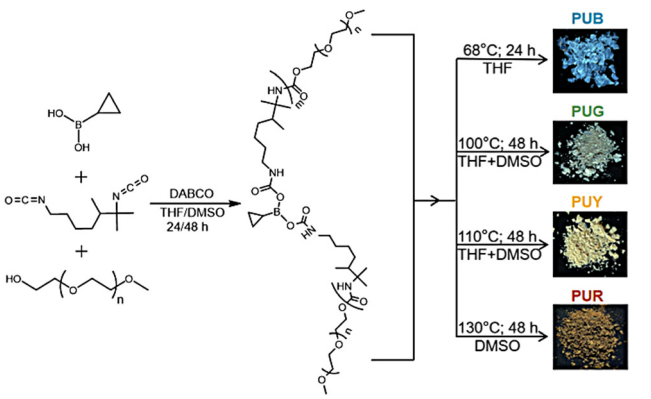

Fig. 1 Synthesis of the PUs and fluorescence photographs of the corresponding powder samples under 365 nm UV illumination (B = blue; G = green; Y = yellow; and R = red).

Results and discussion

Synthesis

By simply regulating the reaction temperature in one-pot reactions, monomolecular multicolour polyurethane derivatives (PUs) **PUB**, **PUG**, **PUY** and **PUR** were obtained. Nuclear magnetic resonance (NMR) spectroscopy shows that the PUs are well-structured materials. Their chemical compositions were shown to be the same (Fig. S1, ESI†). However, their –NH peak positions were different, suggesting that their different luminescence properties might come from the differences in hydrogen bonding patterns. The characteristic peaks in the FT-IR spectra also demonstrate the successful synthesis of the PUs (Fig. S2, ESI†). The molecular weight of the PUs is studied by gel permeation chromatography (GPC) (Table S2, ESI†), and the optical results show that luminescence gradually changed from blue to yellow with the increase in the molecular weight. The above results show that the PUs are molecular weight-dependent polychromatic luminescent materials. It is strange that the molecular weight of **PUR** was slightly reduced compared to those of **PUB**, **PUG** and **PUY**, which may be because the high reaction temperature makes the addition polymerisation to occur too rapidly, which is not conducive to the generation of long-chain segments. However, a higher temperature intensifies the aggregation of the polymer chains, so **PUR** shows the longest wavelength (red-light) emission.

Photophysical characterisation of PUs

The solid-state absorption spectra of the PUs and cyclopropyl boric acid monomer are shown in Fig. S3 (ESI†). As the reaction temperature increases, the spectrum of the PUs gradually widens and extends to longer wavelengths that are more favourable for light absorption. As the reaction temperature increases, the PU chain structure gradually changes from a relatively free state to a weakly aggregated state, and then to a strongly aggregated state. The latter state will significantly promote the through-space conjugation of electrons, thus narrowing the energy level gap.[32] Indeed, as the energy gap decreases from 3.22 eV to 1.51 eV, the emission redshifts and widens (Fig. S3 and S4a, ESI†). Due to the lack of any large π-conjugated units, these PUs are clusteroluminescent materials.[17] As seen in Fig. S5 (ESI†), the PUs all show typical excitation dependence characteristics; their emission gradually moved towards longer wavelengths with the increase of an excitation wavelength. To probe the excitation dependence in more detail, the PUs were studied by fluorescence microscopy. As shown in Fig. 2, fascinating colourful emission behaviour was observed at different excitation wavelengths and emission acquisition bands. This implies the existence of different emission species in the PU system, which will be discussed in detail at the later part of this section.

Unexpectedly, **PUY** has a remarkable ultra-long room temperature phosphorescence (RTP) lifetime observed by the

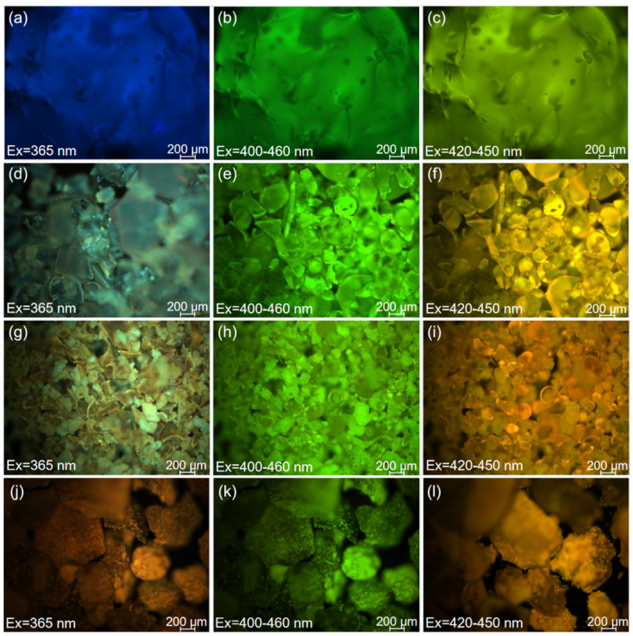

Fig. 2 Fluorescence microscopy images of (a)–(c) **PUB**, (d)–(f) **PUG**, (g)–(i) **PUY** and (j)–(l) **PUR** in the solid state.

naked eye over 3 s at room temperature. The time-resolved spectrum (Fig. 3(a)) shows that in the phosphorescence mode, **PUY** emitted at a λ_{max} of 550 nm. After the light source was turned off, the emission redshifted to a λ_{max} of 603 nm, and the phosphorescence lifetime was 0.45 s (Fig. 3(b) and ESI,† Video 1). Like the steady-state fluorescence spectrum, the phosphorescence spectrum also shows excitation dependence in the 400–800 nm range at excitation wavelengths λ_{ex} of 325–565 nm (Fig. S6, ESI†). These data further suggest that there are a variety of emission aggregates in the PU system that can be excited by the excitation light of different energies.[2,11–13,27,51–53]

To gain insight into the phosphorescence mechanism of **PUY**, the emission spectra of **PUY** powders at 77 K were characterised. As shown in Fig. S7a (ESI†), the phosphorescence of **PUY** at 77 K is red-shifted compared to room temperature, while maintaining excitation dependent properties (Fig. S7b, ESI†). From the steady-state spectra at 298 K and 77 K (Fig. S7a, ESI†) there is a small energy gap (0.32 eV) between the S_1 and T_1 states, which can promote the ISC and reverse intersystem crossing (RISC) processes between S_1 and T_1, thereby extending the exciton lifetime.[20] The influence of trace residues such as monomers and catalysts on NCLPs' luminescence is controversial. For this reason, the emission spectra of the cyclopropyl boronic acid monomer and the catalyst DABCO were collected at varying excitation wavelengths. The PL spectra showed no long-wavelength emission except for interference (Fig. S8, ESI†).[52]

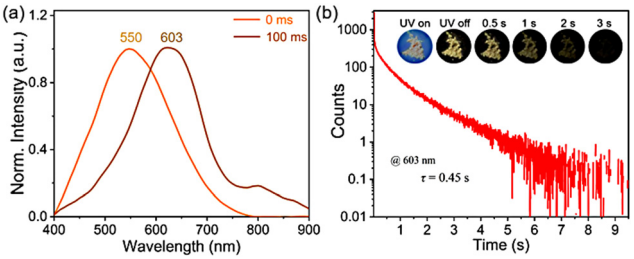

Fig. 3 (a) Time-resolved delayed spectra of the **PUY** powder sample. (b) Lifetime curve of **PUY**. Inset: Phosphorescence images of **PUY** under a 365 nm UV lamp.

To better explain the excitation dependent emission principle of PUs, the emission lifetime of **PUY** was collected at different excitation wavelengths at 298 K. As shown in Fig. S9a (ESI†), at λ_{ex} of 365 nm and 405 nm **PUY** emits RTP with lifetimes of 0.34 s and 0.36 s at 550 nm and 568 nm, respectively. In addition, the lifetime of **PUY** in the steady-state spectrum at 77 K has also been studied (Fig. S9b, ESI†), with the main peak at 554 nm having a lifetime of 0.70 s under 365 nm excitation, and the shoulders at 366 nm and 401 nm having lifetimes of 0.37 s and 0.38 s, respectively. The above photophysical characterisation results prove that the excitation dependent characteristics come from different emission species, which is a major feature of non-conjugated polymers.[11–16] As the absorption range of PUs after polymerisation is greatly expanded (Fig. S3, ESI†), different aggregation chain segments can be excited by light of different wavelengths, so the PUs can present different emissions under different excitation conditions.

Morphological properties of PUs

In the wide-angle X-ray diffraction (WAXD) experiments (Fig. S10, ESI†), all four samples show broad peaks at about 20°, which is the characteristic of a polyurethane skeleton.[53] However, the peaks are of different intensities and widths, indicating that the interchain hydrogen bonding interactions differ in these PU samples, indicating that the PUs have different stacking structures. To establish the microscopic aggregation behaviour, scanning electron microscopy (SEM) images were obtained.

As shown in Fig. 4, **PUB** has a sparse nanosphere structure. With the increasing molecular weight, **PUG** has large-sized nanowire aggregates and **PUY** shows a dense super-clustered structure. At the same time, the luminous efficiency of **PUY** (3.3%) is also the highest among this series (Table S3, ESI†). However, **PUR**, which has the highest reaction temperature during the preparation process, presents a flat sheet structure.

A high temperature is conducive to the PU chain segments tending to aggregate,[54] so **PUR** presents the most red shifted luminescence among the PUs at 130 °C. However, according to the mechanism of addition polymerisation, excessive temperature is not conducive to the formation of long chain segments; therefore, **PUR** has the lowest molecular weight among the PUs. In addition, it is noted in Fig. S5 (ESI†) that only the excitation dependence characteristics of **PUR** are greatly reduced. This also corresponds to the microstructure of the PUs observed in Fig. 4. Compared with the nanosphere/nanowire/supernanocluster aggregation structure of the other three products, only **PUR** presents a large-sized flat sheet structure, which we speculate that it is very unfavourable to electron conjugation in non-traditional chromophores and will not lead to the

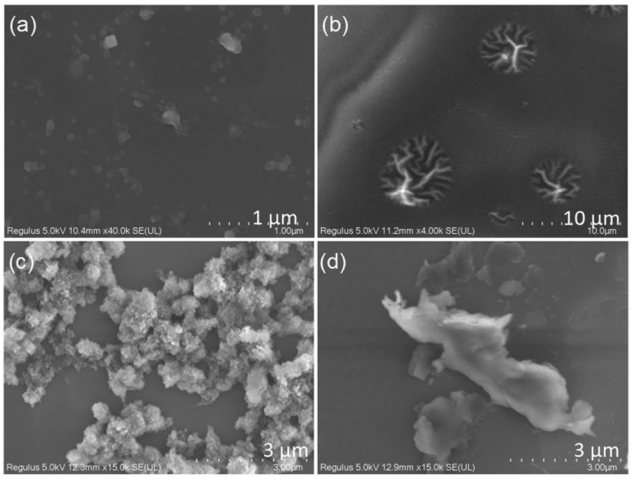

Fig. 4 SEM images of (a) **PUB**, (b) **PUG**, (c) **PUY** and (d) **PUR** in ethanol (20 mg mL^{-1}).

formation of multiple kinds of luminous clusters. Besides, from Fig. S5 and Table S3 (ESI†), it can be concluded that although this kind of high-temperature polymerisation can redshift the emission of PUs without affecting the luminous intensity, it may be that the high temperature makes the polymer chain segments too bent and twisted (Fig. S10d, ESI†) which is not conducive to the luminous efficiency.

For NCLPs, the final aggregation structure is more influential than the isolated chemical structure on the photophysical properties of the material.[35,36,40,52,53] Thus, although the PUs have the same chemical structure, they show different microscopic aggregation structures due to different molecular conformation and aggregation behaviour (Fig. 4). Combining the microscopy results and the photophysical data above, we propose that tight nanoaggregated structures effectively increase the conjugation and redshift the emission. Compared with the flat sheet structure, the dense super-cluster aggregation is more conducive to the through-space conjugation of the electron clouds, thus promoting the spin–orbit coupling and ISC processes, and finally obtaining the ultra-long phosphorescence of **PUY**. Among PUs, only **PUY** has a super-cluster microscopic conformation: this structure allows the chromophore units to approach each other more freely, thereby increasing the chance of contact between the lone pair electrons and the π electrons, which further enhances electron delocalisation, finally obtaining excellent ultra-long RTP. This will be further discussed in detail in the luminescence mechanism studies below.

Mechanism of luminescence

To probe the multicolour luminescence mechanism of PUs, the highest occupied and lowest unoccupied molecular orbital (HOMO and LUMO, respectively) levels of the PUs were studied by cyclic voltammetry (CV).[55] Fig. S11 and S12 (ESI†) show the CV curves of **PUB**, **PUG**, **PUY** and **PUR** and the corresponding calculated HOMO and LUMO levels. Table S4 (ESI†) summarises the E_{HOMO} and E_{LUMO} values. These results further prove that with the increasing reaction temperature, the HOMO–LUMO gaps gradually decreases, which is consistent with the emission trend in Fig. S4a (ESI†). Luminous clusters with new orbitals diversify the HOMO–LUMO gaps after aggregation and give rise to the remarkably colourful luminescence of the PUs and to the ultra-long phosphorescence of **PUY**.

To further explore the clusteroluminescence mechanism, density functional theory (DFT) was used to optimise the conformation of the PUs based on two repeating units at the B3LYP/6-31G(d) level. Fig. S13 (ESI†) shows the HOMO/LUMO electron clouds. The data show that through-space conjugation exists in the PUs.[56] Fig. S14 (ESI†) shows that there are a large number of hydrogen bonding interactions (such as C–H···O═C, C–H···N and N–H···N), through-space dative bonds (carbonyl oxygen/ether oxygen to B atoms) and short contacts.[57–59] Table S5 (ESI†) shows the many short-range O···O interactions, suggesting that many oxygen clusters exist, which would facilitate the overlap of electron clouds, then enhancing spatial conjugation, rigidifying the conformation, and finally stabilising excitons.[36]

To evaluate the interatomic interactions more accurately, the Materials Studio software was used to build the equilibrated model of the PUs (Fig. S15 and Video 2, ESI†). The simulation box is shown to represent periodic boundaries. 35 molecules were invested in the construction process, resulting in a total of 10 AC boxes. The structure was then subjected to 10 000 energy-minimisation iterations using the smart algorithm to rule out unreasonable contact situations, such as overlapping parts and overly dense contact between molecules. More details are included in the ESI.† The radial distribution function $g(r)$ of boron (B) and oxygen (O) was obtained by molecular dynamics simulations. The radial distribution function (RDF) analysis shows that there are many through-space coordination interactions between boron and oxygen atoms in the PUs, which would facilitate the luminescence behaviour. The intermolecular interactions of B and O atoms are shown in Fig. 5(a) inset images. As shown in Fig. 5(a), the position corresponding to the first peak value is consistent with a distance of 1.444 Å between B and adjacent O atoms in the single molecule optimised by the DFT calculations in Fig. 5(a), suggesting that there are a large number of strong B···O short-range spatial correlations within the PU molecules. In addition, from the corresponding positions of the second and third peaks, the distance between the B and O atoms is in the range of 2.91 to 3.57 Å, which is smaller than the corresponding van der Waals distance (3.65 Å). A maximum distance of 3.57 Å is derived from the distance between the B and O atoms (Fig. 5(a)).

There are extensive and complex interactions between the PU chains. Overall, the synergistic effects of non-covalent interactions, oxygen clusters and through-space dative bonds enable the PUs to form and stabilise various luminescent clusters, resulting in the splitting and coupling of the molecular orbitals, the generation of new molecular orbitals and ISC channels,[60] culminating in the excitation-dependent properties and the remarkable ultra-long phosphorescence, as shown in Fig. 5(b).

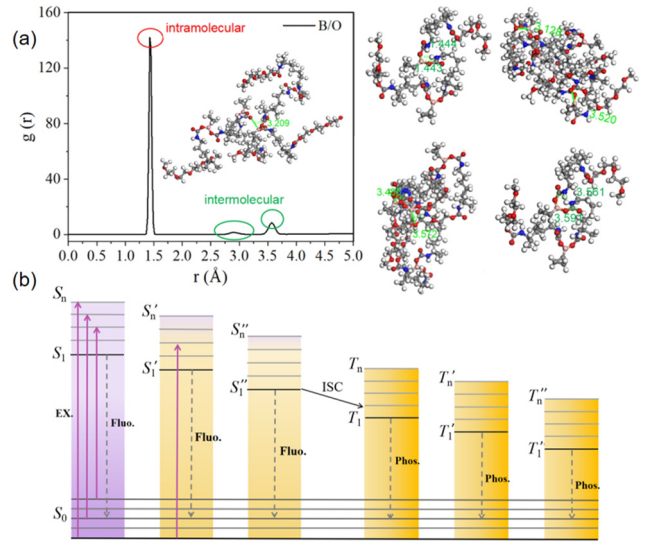

Fig. 5 (a) Radial distribution functions of B and O atoms in PUs by molecular dynamics simulations. Inset: The average inter- or/and intra-chain distance between the B and O atoms in the PUs (C-gray; H-white; N-blue; O-red; and B-pink). (b) Jablonski diagram explains the multicolour emissions and ultra-long phosphorescence of PUs.

In addition, the spin–orbit coupling (SOC) constant between the S_1 state and the T_n state has been calculated using ORCA 5.0.3 after the S_1 state was optimised with Gaussian 16. As shown in Table S6 (ESI†), the PUs possess very large SOC coefficients, which will undoubtedly contribute to the more active electron-exchange.[61–63] Strangely, under such a premise, only **PUY** has phosphorescence properties. It can be seen that for NCLPs that emit by electron cloud conjugation, the microscopic aggregation structure that the materials eventually adopt is a decisive factor in determining their final properties.

Applications

RTP materials have unique advantages in the fields of advanced information storage and transmission. To demonstrate a practical application of the PUs, two proof-of-concept information transmission models were prepared. Fig. 6(a) shows an advertising board for socks. The red socks were painted with **PUR**, and letters S and O were painted with **PUY** and letters C and K were painted with another polyurethane material with similar fluorescence to **PUY**. When the ultraviolet light was turned on, the word "SOCKS" was displayed; however, when the UV light was turned off, the emergency "SOS" distress message was revealed. Fig. 6(b) shows an information storage and the transmission model based on the Morse code. Dots and lines were painted with **PUY** and with another polyurethane material with similar fluorescence to **PUY**. Different combinations of dots and lines represent different letters. When the UV light was turned on, the fluorescence code was decoded as the general information "FORK", but after turning off the UV light, the phosphorescence code sent an "SOS" message.

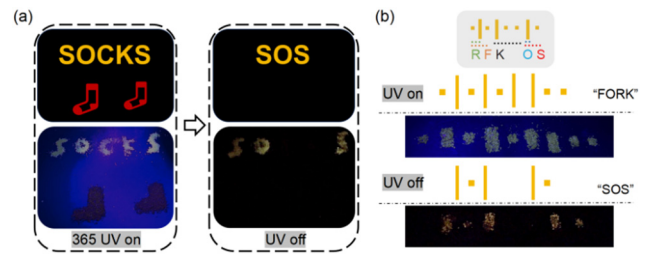

Fig. 6 The application of PUs for encrypted information transfer models. (a) Schematic diagram of an advertising board. (b) Schematic diagram of the Morse code.

Conclusions

In summary, electron-deficient boron atoms have been introduced into polyurethane main chains. The resulting PUs (**PUB**, **PUG**, **PUY** and **PUR**), which have no aromatic rings or traditional chromophore units or heavy atoms, show multicolour emission (blue, green, yellow and red) relying solely on regulatory molecular aggregation. The main breakthrough is that **PUY** also exhibits an ultra-long room temperature phosphorescence lifetime of 0.45 s which (to our knowledge) is the longest lifetime for pure NCLPs reported to date. In-depth experimental and theoretical analyses have shown that the synergy of inter/intra-molecular hydrogen bonds, through-space dative bonds and oxygen clusters is the root cause of multicolour fluorescence and ultra-long phosphorescence. The results have important implications for understanding the intrinsic mechanism of unconventional luminescence in the absence of any traditional conjugative units or heavy atom effects. This work demonstrates new horizons for NCLPs with simultaneous panchromatic emission and ultra-long RTP. Furthermore, a proof-of-concept demonstration of the new PUs in information storage and multi-level encryption paves the way for enhanced properties and applications of NCLPs by fine-tuning the structural morphology. PU derivatives are topical for these future studies as progress is being made in their use as an eco-friendly alternative to non-biodegradable plastics.[64]

Author contributions

Conceptualisation: N. Jiang and Y.-H. Xu. Synthesis: K.-X. Li. Theoretical calculations: J.-J. Wang and N. Jiang. Investigation: N. Jiang and M. R. Bryce. Characterisation: K.-X. Li, C.-S. Li and X.-Y. Xu. Writing, reviewing and editing: N. Jiang, Y.-H. Xu and M. R. Bryce.

Conflicts of interest

The authors declare that they have no known competing financial interests or personal relationships that could have appeared to influence the work reported in this paper.

Acknowledgements

This work was funded by the Science and Technology Development Program of Jilin Province (YDZJ202301ZYTS305), the Research Program on Science and Technology from the Education Department of Jilin Province (grant no. JJKH20220433KJ), and the NSFC (grant no. 21975103). M. R. B. thanks the EPSRC grant EP/L02621X/1 for funding. You-Liang Zhu at Supramolecular Structure and Materials, College of Chemistry, Jilin University, Changchun, 130012, China is thanked for help with the molecular dynamics simulation.

Notes and references

1 H. J. Kim, C. Lee, M. Godumala, S. Choi, S. Y. Park, M. J. Cho, S. Park and D. H. Choi, *Polym. Chem.*, 2018, **9**, 1318–1326.
2 Z. A. Page, C. Y. Chiu, B. Narupai, D. S. Laitar, S. Mukhopadhyay, A. Sokolov, Z. M. Hudson, R. Bou Zerdan, A. J. McGrath, J. W. Kramer, B. E. Barton and C. J. Hawker, *ACS Photonics*, 2017, **4**, 631–641.
3 Z. Wang, X. Zou, Y. Xie, H. Zhang, L. Hu, C. C. S. Chan, R. Zhang, J. Guo, R. T. K. Kwok, J. W. Y. Lam, I. D. Williams, Z. Zeng, K. S. Wong, C. D. Sherrill, R. Ye and B. Z. Tang, *Mater. Horiz.*, 2022, **9**, 2564–2571.
4 C. Weng, N. Fan, T. Xu, H. Chen, Z. Li, Y. Li, H. Tan, Q. Fu and M. Ding, *Chin. Chem. Lett.*, 2020, **31**, 1490–1498.
5 L. Guo, L. Yan, Y. He, W. Feng, Y. Zhao, B. Z. Tang and H. Yan, *Angew. Chem., Int. Ed.*, 2022, **61**, e202204383.
6 B. Han, Q. Yan, Z. Xin, Q. Liu, D. Li, J. Wang and G. He, *Aggregate*, 2022, **3**, e147.
7 B. Sui, Y. Li and B. Yang, *Chin. Chem. Lett.*, 2020, **31**, 1443–1447.
8 J. Mun, G. N. Wang, J. Y. Oh, T. Katsumata, F. L. Lee, J. Kang, H. Wu, F. Lissel, S. Rondeau Gagné, J. B. H. Tok and Z. Bao, *Adv. Funct. Mater.*, 2018, **28**, 1804222.
9 S. Chen, L. Yin, L. Liu, N. Zhang and D. Dong, *Chin. Chem. Lett.*, 2021, **32**, 3133–3136.
10 B. Liu, B. Chu, Y. Wang, Z. Chen and X. Zhang, *Adv. Opt. Mater.*, 2020, **8**, 1902176.
11 Z. Zhang, Z. Xiong, B. Chu, Z. Zhang, Y. Xie, L. Wang, J. Z. Sun, H. Zhang, X. Zhang and B. Z. Tang, *Aggregate*, 2022, **3**, e278.
12 Z. Wang, H. Zhang, S. Li, D. Lei, B. Z. Tang and R. Ye, *Top. Curr. Chem.*, 2021, **379**, 14.
13 S. Tang, T. Yang, Z. Zhao, T. Zhu, Q. Zhang, W. Hou and W. Z. Yuan, *Chem. Soc. Rev.*, 2021, **50**, 12616–12655.
14 B. Song, J. Zhang, J. Zhou, A. Qin, J. W. Y. Lam and B. Z. Tang, *Nat. Commun.*, 2023, **14**, 3115.
15 T. Yang, J. Zhou, B. Shan, L. Li, C. Zhu, C. Ma, H. Gao, G. Chen, K. Zhang and P. Wu, *Macromol. Rapid Commun.*, 2022, **43**, 2100720.
16 Y. Z. Fan, L. Han, Y. Z. Yang, Z. Sun, N. Li, B. L. Li, H. Q. Luo and N. B. Li, *Environ. Sci. Technol.*, 2020, **54**, 10270–10278.
17 Y. L. Wang, K. Chen, H. R. Li, B. Chu, Z. Yan, H. K. Zhang, B. Liu, S. Hu and Y. Yang, *Chin. Chem. Lett.*, 2023, **34**, 107684.
18 S. Wang, D. Wu, S. Yang, Z. Lin and Q. Ling, *Mater. Chem. Front.*, 2020, **4**, 1198–1205.
19 X. H. Chen, Y. Z. Wang, W. Z. Yuan and Y. M. Zhang, *Prog. Chem.*, 2019, **31**, 1560–1575.
20 D. Li, Y. Yang, J. Yang, M. Fang, B. Z. Tang and Z. Li, *Nat. Commun.*, 2022, **13**, 347.
21 H. Ma, Q. Peng, Z. An, W. Huang and Z. Shuai, *J. Am. Chem. Soc.*, 2019, **141**, 1010–1015.
22 B. Zhao, S. Yang, X. Yong and J. Deng, *ACS Appl. Mater. Interfaces*, 2021, **13**, 59320–59328.
23 Y. Gong, Y. Tan, J. Mei, Y. Zhang, W. Yuan, Y. Zhang, J. Sun and B. Z. Tang, *Sci. China: Chem.*, 2013, **56**, 1178–1182.
24 P. Baronas, R. Komskis, E. Tankelevičiūtė, P. Adomėnas, O. Adomėnienė and S. Juršėnas, *J. Phys. Chem. Lett.*, 2021, **12**, 6827–6833.
25 Y. Xiong, Z. Zhao, W. Zhao, H. Ma, Q. Peng, Z. He, X. Zhang, Y. Chen, X. He, J. W. Y. Lam and B. Z. Tang, *Angew. Chem., Int. Ed.*, 2018, **57**, 7997–8001.
26 C. Ren, Z. Wang, T. Wang, J. Guo, Y. Dai, H. Yuan and Y. Tan, *Chin. J. Chem.*, 2022, **40**, 1987–2000.
27 K. Chen, Y. Wang, B. Chu, Z. Yan, H. Li, H. Zhang, S. Hu, Y. Yang, B. Liu and X. H. Zhang, *J. Mater. Chem. C*, 2022, **10**, 16420–16429.
28 Z. He, H. Gao, S. Zhang, S. Zheng, Y. Wang, Z. Zhao, D. Ding, B. Yang, Y. Zhang and W. Z. Yuan, *Adv. Mater.*, 2019, **31**, 1807222.
29 Y. F. Zhang, Y. Su, H. W. Wu, Z. H. Wang, C. Wang, Y. Zheng, X. Zheng, L. Gao, Q. Zhou, Y. Yang, X. H. Chen, C. L. Yang and Y. L. Zhao, *J. Am. Chem. Soc.*, 2021, **143**, 13675–13685.
30 Y. Wang, X. Bin, X. Chen, S. Zheng, Y. Zhang and W. Z. Yuan, *Macromol. Rapid Commun.*, 2018, **39**, 1800528.
31 B. Zhao, S. Yang, X. Yong and J. Deng, *ACS Appl. Mater. Interfaces*, 2021, **13**, 59320–59328.
32 H. Zhang, Z. Zhao, P. R. McGonigal, R. Ye, S. Liu, J. W. Y. Lam, R. T. K. Kwok, W. Z. Yuan, J. Xie, A. L. Rogach and B. Z. Tang, *Mater. Today*, 2020, **32**, 275–292.
33 B. Chu, H. Zhang, K. Chen, B. Liu, Q. L. Yu, C. J. Zhang, J. Sun, Q. Yang, X. H. Zhang and B. Z. Tang, *J. Am. Chem. Soc.*, 2022, **144**, 15286–15294.
34 J. Chen, Q. Peng, X. Peng, H. Zhang and H. Zeng, *Chem. Rev.*, 2022, **122**, 14594–14678.
35 B. Liu, B. Chu, L. Zhu, H. Zhang, W. Z. Yuan, Z. Zhao, W. M. Wan and X. H. Zhang, *Chin. Chem. Lett.*, 2023, **34**, 107909.
36 B. Chu, H. Zhang, L. Hu, B. Liu, C. Zhang, X. Zhang and B. Z. Tang, *Angew. Chem., Int. Ed.*, 2022, **61**, e202114117.
37 D. Wang, X. Wang, C. Xu and X. Ma, *Sci. China: Chem.*, 2019, **62**, 430–433.
38 X. Dou, Q. Zhou, X. Chen, Y. Tan, X. He, P. Lu, K. Sui, B. Z. Tang, Y. Zhang and W. Z. Yuan, *Biomacromolecules*, 2018, **19**, 2014–2022.
39 P. Han, G. Zhang, J. Wang, Y. Yao, Y. Qiu, H. Xu, A. Qin and B. Z. Tang, *CCS Chem.*, 2023, **5**, 1686–1696.

40 W. Li, W. Zhou, Z. Zhou, H. Zhang, X. Zhang, J. Zhuang, Y. Liu, B. Lei and C. Hu, *Angew. Chem., Int. Ed.*, 2019, **58**, 7278–7283.
41 H. E. Hackney and D. F. Perepichka, *Aggregate*, 2022, **3**, e123.
42 X. Li, R. Shimaya, T. Dairi, W. Chang and Y. Ogasawara, *Angew. Chem., Int. Ed.*, 2022, **61**, e202113189.
43 H. Meng, M. S. Liu and W. Shu, *Chem. Sci.*, 2022, **13**, 13690–13707.
44 M. J. Kim, D. J. Wang, K. Targos, U. A. Garcia, A. F. Harris, I. A. Guzei and Z. K. Wickens, *Angew. Chem., Int. Ed.*, 2023, **62**, e202303032.
45 Z. An, C. Zheng, Y. Tao, R. Chen, H. Shi, T. Chen, Z. Wang, H. Li, R. Deng, X. Liu and W. Huang, *Nat. Mater.*, 2015, **14**, 685–690.
46 Z. Yang, Z. Mao, X. Zhang, D. Ou, Y. Mu, Y. Zhang, C. Zhao, S. Liu, Z. Chi, J. Xu, Y. C. Wu, P. Y. Lu, A. Lien and M. R. Bryce, *Angew. Chem., Int. Ed.*, 2016, **55**, 2181–2185.
47 X. Chen, T. Yang, J. Lei, X. Liu, Z. Zhao, Z. Xue, W. Li, Y. Zhang and W. Z. Yuan, *J. Phys. Chem. B*, 2020, **124**, 8928–8936.
48 Q. Zhou, Z. Wang, X. Dou, Y. Wang, S. Liu, Y. Zhang and W. Z. Yuan, *Mater. Chem. Front.*, 2019, **3**, 257–264.
49 S. Zheng, T. Hu, X. Bin, Y. Wang, Y. Yi, Y. Zhang and W. Z. Yuan, *ChemPhysChem*, 2020, **21**, 36–42.
50 F. Kausar, Z. Zhao, T. Yang, W. Hou, Y. Li, Y. Zhang and W. Z. Yuan, *Macromol. Rapid Commun.*, 2021, **42**, 2100036.
51 Y. Zhang, H. Yang, H. Ma, G. Bian, Q. Zang, J. Sun, C. Zhang, Z. An and W. Wong, *Angew. Chem., Int. Ed.*, 2019, **58**, 8773–8778.
52 Z. Zhang, J. Zhang, Z. Xiong, B. Chu, C. Zhang, J. Z. Sun, H. Zhang, X. Zhang and B. Z. Tang, *Angew. Chem., Int. Ed.*, 2023, **135**, e202306762.
53 N. Jiang, S. H. Ruan, X. M. Liu, D. Zhu, B. Li and M. R. Bryce, *Chem. Mater.*, 2020, **32**, 5776–5784.
54 H. Fu, H. Gao, G. Wu, Y. Wang, Y. Fan and J. Ma, *Soft Matter*, 2011, **7**, 3546–3552.
55 X. Yin, F. Guo, R. A. Lalancette and F. Jäkle, *Macromolecules*, 2016, **49**, 537–546.
56 J. Deng, Y. Bai, J. Li, J. Jiang, C. Zhao, W. Xie, Y. Guo, H. Liu, D. Liu, L. Yu and H. Wang, *Adv. Opt. Mater.*, 2023, 2300715.
57 G. J. Bartlett, A. Choudhary, R. T. Raines and D. N. Woolfson, *Nat. Chem. Biol.*, 2010, **6**, 615–620.
58 R. W. Newberry and R. T. Raines, *Chem. Commun.*, 2013, **49**, 7699–7701.
59 R. W. Newberry and R. T. Raines, *Acc. Chem. Res.*, 2017, **50**, 1838–1846.
60 Q. Wang, X. Dou, X. Chen, Z. Zhao, S. Wang, Y. Wang, K. Sui, Y. Tan, Y. Gong, Y. Zhang and W. Z. Yuan, *Angew. Chem., Int. Ed.*, 2019, **58**, 12667–12673.
61 C. A. M. Salla, G. Farias, M. Rouzières, P. Dechambenoit, F. Durola, H. Bock, B. de Souza and I. H. Bechtold, *Angew. Chem., Int. Ed.*, 2019, **58**, 6982–6986.
62 G. Farias, C. A. M. Salla, M. Aydemir, L. Sturm, P. Dechambenoit, F. Durola, B. de Souza, H. Bock, A. P. Monkman and I. H. Bechtold, *Chem. Sci.*, 2021, **12**, 15116–15127.
63 S. Hirata, *Adv. Opt. Mater.*, 2017, **5**, 1700116.
64 M. Mangal, C. V. Rao and T. Banerjee, *Polym. Int.*, 2023, **72**, 984–996.